

Adopting the Multiresolution Wavelet Analysis in Radial Basis Functions to Solve the Perona-Malik Equation

A. Khatoon Abadi¹, K. Yahya², M. Amini^{*1}

¹ Department of Mathematics, Faculty of Mathematical Sciences, Tarbiat Modares University, Tehran 14115-134, Islamic Republic of Iran

² Faculty of Informatics, Chemnitz University of Technology, Straße der Nationen 62|R. B216, 09111 Chemnitz, Germany

Received: 13 June 2018 / Revised: 30 July 2018 / Accepted: 11 August 2018

Abstract

Wavelets and radial basis functions (RBF) have ubiquitously proved very successful to solve different forms of partial differential equations (PDE) using shifted basis functions, and as with the other meshless methods, they have been extensively used in scattered data interpolation. The current paper proposes a framework that successfully reconciles RBF and adaptive wavelet method to solve the Perona-Malik equation in terms of locally shifted functions. We take advantage of the scaling functions that span multiresolution subspaces to provide resilient grid comprising centers. At the next step, the derivatives are computed and summed over these local feature collocations to generate the solution. We discuss the stability of the solution and depict how convergence could be granted in this context. Finally, the numerical results are provided to illustrate the accuracy and efficiency of the proposed method.

Keywords: Adaptive wavelet method; Radial basis functions; Perona-Malik equation.

Introduction

Originating from neural networks and learning, Radial Basis Functions (RBF) has penetrated a variety of computational tasks ranging from supervised learning (making input-output comparison) and support vector machine classification [1,2] to the interpolation of scattered sampled data and image restoration [3,4]. As with other meshless methods, RBF have been frequently used for the numerical solution of PDEs and their extensive use in numerical analysis prompted us to investigate the possibility of their combination with wavelets to provide the numerical solution for ill-made anisotropic diffusion PDEs in general and Perona-Malik equation as a powerful method of image processing.

Perona-Malik equation is studied using different methods, including fixed point method [5]. The equation is important because of its applications in image enhancement (see e.g. [6]). It is also used as a model for image denoising [7] and shape detection [8,9].

After giving a brief description of the formal structures of RBF together with multiresolution wavelet analysis (MRWA) in the first section, we will devote the rest of the paper to elaborate on having these two methods (despite their essential difference in locality) funneled to reach a fulfilling approximation for the Perona-Malik equation. It is worth mentioning that the main idea behind our work is to exploit the wavelet basis so as to generate the solution state and refine the

* Corresponding author: Tel: +982182883416; Fax: +982182883416; Email: mamini@modares.ac.ir

established RBF centers whereupon the derivatives are computed at each step. As it will be shown, the latter (backward computation of the derivatives over the transient centers) is somehow similar to using the power series in solving differential equations. It should be noted that because this strategy is rapidly growing among the literature we avoid taking any comprehensive approach and instead try to demonstrate how it already has gained superiority over its counterparts.

In recent years, few methods have been suggested to combine RBF and wavelets in different forms. Categorically we could divide the whole body of the literature into two sections. Some of the suggested methods attempt to apply the wavelet in refining-coarsening the RBF algorithms whereas the others try to produce new types of wavelets via employing RBF as the basis instead of the well-known usual ones. In the first category, most of the work are mainly concentrated on enhancing the adaptivity of RBF centers. For example, Vrankar et. al. [10] proposed a method to solve time dependent moving boundary problems by the virtue of the wavelet style refinement techniques, which use wavelets to define a greedy RBF algorithm that captures and tracks the changes along the contours. In the second category, we could also point out a method called ‘central basis function’ that was produced in [11] presenting a model that yields conventional multiresolution wavelet bases through shifting one side functions including RBF. This paper too belongs to the first category in regard to its scope, method and materials.

Given a radially symmetric function $\phi(x) = \phi(\|x\|)$ we can define a radial basis function as follows:

$$f(x) = \sum_k \lambda_k \phi(\|x - x_k\|),$$

where $\|x - x_k\|_2$ is the Euclidean distance between $x \in \mathbb{R}^d$ and $x_k \in \mathbb{R}^d$ (called center, typically one for each nodal point) and it implies that the value of the function ϕ and thus the interpolant f solely depends on the distance of the trajectory that links x to x_k . Furthermore, we have a class of radially symmetric functions among which the following forms are more popular.

$$\begin{aligned} \phi(r) &= 1/(1 + c^2 r^2), && \text{Reciprocal} \\ \phi(r) &= \sqrt{1 + c^2 r^2}, && \text{Multiquadratic} \\ \phi(r) &= r^2 \log r, && \text{Thin-plate} \end{aligned}$$

Here, c is a constant for shape parameter. Like any classic interpolation method, we have a set of auxiliary points, which are to help us find the appropriate constants λ_k that yield the best approximation. In other words, the main scope of this scheme is more of a finding a solution for a linear $n \times n$ system of equations

$$A = z^T f,$$

where $A_{ij} = \phi_i(x_j)$, $z = [\lambda_1, \dots, \lambda_N]$ and $f = [f_1, \dots, f_N]$, and z^T is the transpose of z . We choose to work with

$$\phi(r) = (1 - r)_+^8 (32r^3 + 25r^2 + 8r + 1),$$

called *wendland polynomial* with compact support, as our basis function. Furthermore, the number of degree of freedom is also tantamount to the number of constraints of the final linear system.

As it can be seen, after picking up a proper basis function as well as setting the linear system (symmetric or asymmetric) the rest is about finding and establishing the centers or nodes. In traditional RBF, the centers usually follow a steady pattern that is poorly suited to our purpose [12]. Considering the nature of our PDE, which is an ill-posed time dependent equation, we need to insert a resilient grid into our computations, so that it can continually update itself with alterations of the equation behavior. Static centers also yield a large number of computations and the solution is more likely to be gained at the expense of optimality [13]. To avoid these difficulties, we shall take an adaptive approach to arrange the centers without working with a large set of points. As we will show, the proposed method can resolve this problem via distributing a set of nodes and shifting them in order to establish the centers around the spots with high gradients, which point out sharp edges in our problem.

Let us briefly review the basic idea behind the discreet wavelet theory (DWT) and *multiresolution analysis* (MRA), both of which are applied to construct our adaptive grid. MRA is an alternative interpolation-representation approach to the Fourier transform, first introduced during the late 80’s and early 90’s by Meyer in [14] (see also, [15]). The pillars of the MRA can be encapsulated in the following propositional scheme. The idea is to expand $L_2(\mathbb{R})$ as the direct sum of the ‘approximation’ subspace $\{V_j\}$ and its orthogonal complement ‘detail’ spaces $\{W_j\}$, where for some appropriate scaling function $\varphi \in L^2(\mathbb{R})$, V_j has an orthonormal basis consisting of the functions

$$\varphi_{jk}(x) = 2^{j/2} \varphi(2^j x - k),$$

as k runs over \mathbb{Z} and W_j is the same thing with φ_{jk} replaced by

$$\psi_{jk}(x) = 2^{j/2} \psi(2^j x - k).$$

These nested subspaces are also invariant under shift but not under translation, namely,

$$\begin{aligned} f(x) \in V_j &\leftrightarrow f(x - k) \in V_j, && f(x) \in V_j \\ &\leftrightarrow f(2x) \in V_{j+1}. \end{aligned}$$

Then $L^2(\mathbb{R})$ can be decomposed as a direct sum of the subspaces W_j .

$$L^2(\mathbb{R}) = \sum_{j \in \mathbb{Z}}^{\oplus} W_j \triangleq \cdots \oplus W_{-1} \oplus W_0 \oplus \cdots$$

and every function $f(x) \in L^2(\mathbb{R})$ will have a unique decomposition

$$f(x) = \cdots + g_{-1}(x) + g_0(x) + g_1(x) + \cdots,$$

where $g_j \in W_j, \forall j \in \mathbb{Z}$. If ψ is regarded as an orthogonal wavelet, then the subspaces $W_j \in L^2(\mathbb{R})$ are mutually orthogonal, $W_j \perp W_l, j \neq l$. For every wavelet ψ (not necessarily orthogonal) we can the following space $V_j \subseteq L^2(\mathbb{R})$

$$\begin{aligned} V_j &= \cdots \oplus W_{-1} \oplus W_0 \cdots \oplus W_{j-2} \oplus W_{j-1}, \\ &= V_0 \oplus W_0 \cdots \oplus W_{j-2} \oplus W_{j-1}. \end{aligned} \quad \text{The}$$

subspaces V_j have the following properties:

1. $\cdots \subseteq V_{-1} \subseteq V_0 \subseteq V_1 \subseteq \cdots$,
2. $\text{clos}_{L^2}(\cup_{j \in \mathbb{Z}} V_j) = L^2(\mathbb{R})$,
3. $\cap_{j \in \mathbb{Z}} V_j = \{0\}$,
4. $V_{j+1} = V_j + W_j, j \in \mathbb{Z}$,
5. $f(x) \in V_j \Leftrightarrow f(2x) \in V_{j+1}, j \in \mathbb{Z}$.

The sequence of subspaces V_j is nested. (see Fig.1) Every $f(x) \in L^2(\mathbb{R})$ can be approximated with any accuracy by the image $P_j f$ of the projection on V_j . If the reference subspace V_0 is generated by a single scaling function $\varphi \in L^2(\mathbb{R})$, then all of the subspaces V_j are also generated by the same function φ , in the same way as the subspaces W_j are generated by the wavelet ψ .

In the multiresolution analysis at a given scale ($j + 1$), the subspaces V_j encode the ‘‘large scale’’ features of the function, whereas the subspaces W_j represents the ‘‘small scale’’ features (details).

Now it follows that every function f can uniquely be represented in terms of the approximating and detailed bases. The approximating wavelet function and its companion detailed function can be both defined with respect to the orthogonality and the nesting properties of the subspaces.

$$\begin{aligned} \phi(x) &= \sqrt{2} \sum_k h_k \varphi(2x - k), \\ \psi(x) &= \sqrt{2} \sum_k g_k \varphi(2x - k), \end{aligned}$$

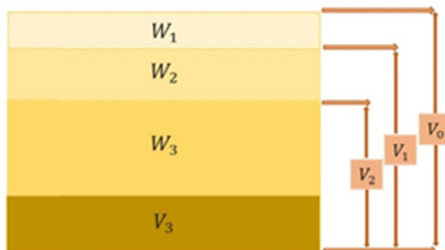


Figure 1. A sequence of multiresolution nested subspaces together with their orthogonal complement can construct the whole space with the finest data resolution

for

$$h_k(x) = 2 \int_{-\infty}^{\infty} \phi(x) \bar{\phi}(2x - k),$$

and similar formula for g_k . The scaling function φ is a two-scale difference function and satisfies the properties $\int_{-\infty}^{\infty} \varphi(x) dx = 1$ and

$$\int_{-\infty}^{+\infty} |\varphi(t)|^2 dt < \infty,$$

representing a band signal, that h_k and g_k can serve as high pass and low pass filters, respectively. These subspaces are compactly supported and therefore data could be transformed from one level of resolution to another. Under the above conditions, we can now represent any given optional function in terms of the bases of the embedded subspaces as follows.

$$u(x) = u^1(x) + u^2(x),$$

where,

$$u^1(x) = \sum_{k=1}^{\infty} \gamma_{j_0,k} \varphi_{j_0,k} + \sum_{j=j_0}^{\infty} \sum_{k=1}^{\infty} \kappa_{j,k} \psi_{j,k},$$

$$u^2(x) = \sum_{j=1}^{j_0} \sum_k \kappa_{j,k} \psi_{j,k}, \eta := \sup_{j,k} \kappa_{j,k} < \infty,$$

in which, the refinement coefficients $\gamma_{j,k} = (u, \varphi_{j,k})$ and $\kappa_{j,k} = (u, \psi_{j,k})$ can be computed as

$$\gamma_{j-1,k} = \sum_l h_{2k-1} \gamma_{j,l} \cdot \kappa_{j-1,k} = \sum_l g_{2k-1} \kappa_{j,l}.$$

Any refinable function φ can uniquely be constructed by a series of refinement coefficients, called mask. Finally, for any smooth function u we will show that there is a threshold $C\zeta$ which puts a bound on the error and guarantees its convergence, that is, $\|u(x) - u^1(x)\|_2 \ll C\zeta$. Note that convergence is derived a theorem that states for all $f \in L_2(\mathbb{R})$, the projection of f on φ , denoted by $P_j f$, converges to f , i.e., $\|P_j f - f\| \rightarrow 0$ in $L_2(\mathbb{R})$ [16]. It is also worth mentioning that for all $f \in L_1(\mathbb{R})$, the convergence is uniform whereas $f \in L_2(\mathbb{R})$, convergence is local and pointwise.

Materials and Methods

In this section, we confine our attention over a group of non-linear anisotropic PDEs which have proven to be very successful in image processing and are thus extensively used in image denoising and deblurring. The common feature of these equations is their striking ability to keep the essential edges and take the control of the speed and intensity of diffusion. Of these equations, we opt for the non-linear version of Perona-Malik equation which is regarded as one of the most cited PDE based works of the field.

Having been adopted as an extended and specific form of the heat-diffusion equation, Perona-Malik equation shared the similar formalism and can be written as follows.

$$\begin{aligned} \partial_t u - \nabla \cdot (g(\|\nabla u^k\|^2)\nabla u) &= 0, \\ u(\vec{x}, 0) &= u_0(\vec{x}), \quad \partial_{\vec{n}} u = 0, \end{aligned}$$

where $u_0(\vec{x})$ is the initial condition at time $t=0$ and $\partial_{\vec{n}} u = 0$ is the Neuman condition. Several numerical solutions based on different methods (such as the finite difference or finite element methods) have been suggested. Here, we will propose a different method and compare the output of to existing results provided by other methods.

First and foremost, it is necessary to offer a discreet form of the equation via replacing that into the RBF system. The aim is to specify the coefficients which are on one hand mediated by MRA and on the other hand vary across the grid. So, we begin with creating a grid that contains the centers. In order to increase the accuracy of our results, we incorporate a more recent form of RBF called adaptive RBF in which centers are locally evaluated in terms of the gradient of the compartment they represent. Centers of high gradients are assessed useful and kept and the rest will be removed. This version of RBF has some certain privileges over the classic form, most importantly, a considerable decreasing of computations that in turn makes the algorithm faster and more optimized. To incorporate adaptive RBF to our method, we need to obtain an initial mesh-free solution upon a base grid first and then distribute it over the nested spaces in order to compute the values of the coefficients at different levels of resolution from the coarsest level to the finest level. In this case, we follow a recursive procedure of refinement and begin with the corset level.

Given the nonlinear PDE as well as its boundary and initial conditions, it is conceivable to start the implementation of the proposed method with spatio-temporal discretization of the solution upon the based grid which is associated with the coarsest level of resolution. We thus set out to employ the collocation method to find the values of the derivatives on N nodes. Spatial discretization is performed by dividing the entire domain Ω into three parts, which are the boundary, boundary condition and Neuman condition, successively (see Fig. 2), namely, $\Omega = \Omega_N + \Omega_l$ where the grid points are given by

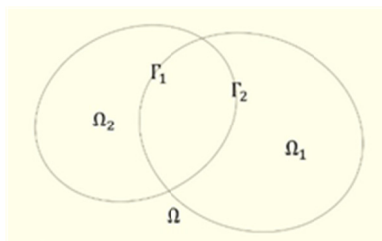


Figure 2. Domain decomposition

$$\begin{aligned} x_i &= ih, \quad i = 0.1. \dots M, \\ t_n &= nk, \quad n = 0.1. \dots N. \end{aligned}$$

Applying θ -scheme will yield the following equations that are discretized in terms of time.

$$\frac{u^k - u^{k-1}}{\tau} = \nabla \cdot (g(\|\nabla u^k\|^2)\nabla u^k).$$

where $\tau = \Delta t$. The right hand side of the above equation can also be expanded and recapped as

$$\begin{aligned} &\nabla \cdot (g(\|\nabla u^k\|^2)\nabla u^k) \\ &= g(\|\nabla u^k\|^2)\nabla^2 u^k \\ &\quad + 2g'(\|\nabla u^k\|^2)D^2 u^k \nabla u^k \cdot \nabla u^k, \end{aligned}$$

which leads to the following system

$$\begin{aligned} &u^{k-1} \\ &= u^k \\ &- \tau(g(\|\nabla u^k\|^2)\nabla^2 u^k \\ &\quad + 2g'(\|\nabla u^k\|^2)D^2 u^k \nabla u^k \cdot \nabla u^k), \quad \text{in } \Omega, \\ &\frac{\partial u^k}{\partial \eta} = 0, \quad \text{on } \Omega. \end{aligned}$$

The system could now be reduced to two main sub systems associated with the subdomains. The approximation of the solution on subdomain Ω_1 at the time step k after n iteration is denoted by $u_1^{k,n}$ whose restriction to the artificial subdomain Γ_2 is also denoted by $u_1^{k,n}|_{\Gamma_2}$. Similarly, the approximation of the solution on Ω_2 at the time step k after n iterations and its restriction to Γ_1 are denoted by $u_2^{k,n}$ and $u_2^{k,n}|_{\Gamma_1}$ respectively. As a result, our boundary value problem will be solved through two inter-related sub problems.

$$\begin{aligned} &u_1^{k-1,n} = u_1^{k,n} - \tau \left(g(\|\nabla u_1^{k,n}\|^2)\nabla^2 u_1^{k,n} + \right. \\ &\quad \left. 2g'(\|\nabla u_1^{k,n}\|^2)D^2 u_1^{k,n} \nabla u_1^{k,n} \cdot \nabla u_1^{k,n} \right), \quad \text{in } \Omega_1, \\ &\frac{\partial u_1^{k-1,n}}{\partial \eta} = 0, \quad \text{on } \partial\Omega_1/\Gamma_1, \\ &u_1^{k,n} = u_2^{k,n-1}|_{\Gamma_1}, \quad \text{on } \Gamma_1, \end{aligned}$$

and,

$$\begin{aligned} &u_2^{k-1,n} = u_2^{k,n} - \tau \left(g(\|\nabla u_2^{k,n}\|^2)\nabla^2 u_2^{k,n} + \right. \\ &\quad \left. 2g'(\|\nabla u_2^{k,n}\|^2)D^2 u_2^{k,n} \nabla u_2^{k,n} \cdot \nabla u_2^{k,n} \right), \quad \text{in } \Omega_2, \\ &\frac{\partial u_2^{k-1,n}}{\partial \eta} = 0, \quad \text{on } \partial\Omega_2/\Gamma_2, \\ &u_2^{k,n} = u_1^{k,n-1}|_{\Gamma_2}, \quad \text{on } \Gamma_2. \end{aligned}$$

For each nodal point, the first and second partial derivatives at each node i and point x are obtained as

$$\begin{aligned} u^1(x) &= \sum_{i=1}^n \phi^1(x)u_i, \\ u^2(x) &= \sum_{i=1}^n \phi^2(x)u_i, \end{aligned}$$

For the $N + L$ moving least squares nodal points as

well as the approximated values of the derivatives, we apply collocation method for all nodal points to gain the following equations.

$$u_j^{k-1} = u_j^k - \tau \left(g \left(\|\nabla u_j^k\|^2 \right) \nabla^2 u_j^k + 2g' \left(\|\nabla u_j^k\|^2 \right) D^2 u_j^k \nabla u_j^k \cdot \nabla u_j^k \right),$$

where

$$u_j^k(x) = \sum_{i=1}^n \phi_i(x_j) u_i^k,$$

$$D^2 u_j^k = \sum_{i=1}^n \left(\frac{\partial \phi_i(x_j)}{\partial x} u_i^k + \frac{\partial \phi_i(x_j)}{\partial y} u_i^k + \frac{\partial^2 \phi_i(x_j)}{\partial x^2} u_i^k + \frac{\partial^2 \phi_i(x_j)}{\partial y^2} u_i^k + \frac{\partial^2 \phi_i(x_j)}{\partial x \partial y} u_i^k \right),$$

$$\nabla^2 u_j^k = \sum_{i=1}^n \left(\phi_i(x_j) + \frac{\partial^2 \phi_i(x_j)}{\partial y^2} \right) u_i^k,$$

satisfying the Neumann condition for the boundary nodes x_j , $j=N+1, \dots, N+L$, for each subdomain, that is,

$$\sum_{i=1}^n \frac{\partial \phi}{\partial \eta}(x_j) u_i^k = 0.$$

To take the whole system forward, we run it recursively with $k=0$, that is associated with our initial condition, $u_j^0 = u^0(x_j)$. Hence, the problem is to solve an algebraic equation system $F^{(k-1)} \mathbf{u}^{(k)} = \mathbf{f}^{(k-1)}$.

$$F_{ij}^{k-1} = \delta_{ij} - \tau \left(g \left(\|\nabla u_j^k\|^2 \right) \sum_{i=1}^n \left(\frac{\partial^2 \phi_j}{\partial x^2}(x_i) + \frac{\partial^2 \phi_j}{\partial y^2}(x_i) \right) + 2g' \left(\|\nabla u_j^k\|^2 \right) \left(\sum_{i=1}^n \left(\frac{\partial \phi_i(x_j)}{\partial x} u_i^k + \frac{\partial \phi_i(x_j)}{\partial y} u_i^k + \frac{\partial^2 \phi_i(x_j)}{\partial x^2} u_i^k + \frac{\partial^2 \phi_i(x_j)}{\partial y^2} u_i^k + \frac{\partial^2 \phi_i(x_j)}{\partial x \partial y} u_i^k \right) \right) \sum_{i=1}^n \left(\frac{\partial^2 \phi_j}{\partial x^2}(x_i) + \frac{\partial^2 \phi_j}{\partial y^2}(x_i) \right) \right),$$

$$f_i^{(k-1)} = u_i^{k-1},$$

We shall reiterate the above procedure until we nail an advisable time step. Then the solution $u(x, t)$ at each point of the domain $x \in \Omega$ could be expressed as $u(x, t) \approx \sum_{i=1}^n \phi_i(x) u_i(t)$, $x \in \Omega$.

Taking an initial solution at the coarsest level, we are going to apply the MRA by distributing it over the nested subspaces. The total account of the proposed

method is that both the smooth features of the picture are attributed to the wavelet coefficients at low levels whereas the highly-localized features are attributed to the wavelet coefficients at higher levels. Any irregularity or variation between the current level and the next coarse level can be depicted by the high values of the wavelet coefficients. It also allows us to make a decision over whether keeping or eliminating any wavelet coefficient that corresponds to some certain node of the domain. Using this adaptation scheme will result in keeping the essential nodes which collectively make a more optimal node distribution.

Results

To provide numerical example, we need to initialize the parameters and opt for a suitable numerical setting of RBF, that is, the type of radial functions we are going to use as well as an optimal node distribution method. To do so, we take into account a case where the system is fed up with the following parameters. We set up $N=698$ (the initial number of collocation nodes), $c = 0.1$ (shape parameter of radial basis functions) and $\varepsilon = 0.001$ (the coarsest level of resolution).

Also, we will separately try both of MQRBF and Wendland polynomial all along our computations and the relevant comparison will be made at the final step. In order to compare the computational, error the l_∞ and RMS norms must be calculated are given as below. l_∞ is a point wise norm taken over the domain while the Root Mean Square (in short RMS) is mean of the squares of the values, usually known for its

stability. We must show that the obtained solution approximates the exact solution of the operator equation (20). In sum, the algorithm that puts the whole system into practice could be elaborated as follows. The numerical results of the adaptive multiresolution wavelet scheme are given in Tables 1 and 2.

The errors are defined by,

$$l_\infty = \text{ess sup} |u^{\text{exact}}(x_i) - u^{\text{app}}(x_i)|,$$

Table 1. Iterative progress of the adaptive multiresolution wavelet scheme (multiquadric function) from level 1 to 4.

N	$\kappa(A)$	l_∞	RMS
320	2.6831e+06	2.27E-02	4.18E-03
732	6.6004e+04	1.53E-01	2.79E-03
756	2.6018e+06	3.14E-02	1.43E-03
764	7.4874e+06	3.23E-03	1.62E-03

Table 2. Iterative progress of the adaptive multiresolution wavelet scheme (Wendland polynomial) from level 1 to 4.

N	$\kappa(A)$	l_∞	RMS
320	7.4352e+04	1.41E+01	1.52E+01
764	2.1255e+06	7.03E-02	7.26E-03
980	6.51E+20	5.24E-01	2.79E-01
1092	1.46E+02	3.92E-02	1.25E-03

Algorithm

Select $S, T \in \mathbb{Z}$
 $T_1 = T/S$
 Put $\Omega_i = [a, b] \times [(i-1)T_1, iT_1], i = 1, 2, \dots, s$
 Set the grid $[a, b] \times [0, T_1]$
 Apply the adaptive MRA
for $j = j_{Max-1} : j_0$ (j 's are all levels of resolution)
for each center of the grid at the j level, $x_{jk}, j, k \in \mathbb{Z}$
Compute: the corresponding wavelet coefficient $\kappa_{j,k}$
 At finer level $j+1, \gamma_{j+1,k}$
 Define ε and apply the adaptive criteria
 If $\kappa_{j,k} < \varepsilon$, then remove $x_{i,k}$ from the grid
 If $\kappa_{j,k} \geq \varepsilon$, the keep $x_{i,k}$ in the grid
 Solve the system
 $\mathbf{F}^{(j-1)} \mathbf{u}^{(j)} = \mathbf{f}^{(j-1)}$
Construct:
 $\mathcal{L} \hat{u}_j(x_i, t_i) = 0, \quad x_i, t_i \in [a, b] \times [0, T_1]$
 $\frac{\partial \hat{u}_j(x_i, t_i)}{\partial \zeta} = 0, x_i, t_i \in [a, b] \times \{0\}$
 Set $L = [l_{ij}], U = [u_{ij}]$ and P =permutation matrix
 Solve $PLU\alpha_1 = f$
 Use forward-backward substitution to find α_1
 Find f_j in $[a, b] \times [(i-1)T_1, iT_1]$
 Use forward-backward substitution to find α_2
 End
 End

Algorithm 1. Algorithmic Solution of the system $\mathbf{F}^{(j-1)} \mathbf{u}^{(j)} = \mathbf{f}^{(j-1)}$.

$$RMS = \sqrt{\frac{1}{N} \sum_{i=1}^N |u^{exact}(x_i) - u^{app}(x_i)|^2}$$

where u^{exact} and u^{app} are the exact and the approximated solutions respectively. Of course, we can define the infinity norm as $l_\infty = \text{ess sup} |u^{exact}(x_i) - u^{app}(x_i)|$.

More details can be found in Fig. 3 in which the error of the area is calculated as a function of time for both of MQRBF and CSRBF.

In addition to the error norms, the accuracy of the

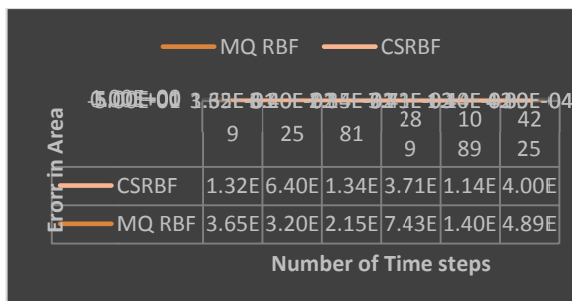


Figure 3. Comparison between errors of two RBFs at different points over time.

method can also be easily evaluated in terms of the order of approximation [17]. Since the definable answer u belongs to the Sobolov space, we need to use some results in Sobolov spaces. Before alluding to those, let us cast a quick glance at the definition of the Sobolov space.

Definition 1. The Sobolev Space H^s of order s is defined by the set of those functions $f(x) \in L^2(\mathbb{R}^d)$ satisfying

$$\|f\|_s \equiv \int_{\Omega} |\hat{f}(x)|^2 (1 + |x|^2)^s dx < \infty$$

The following results could be used for the error analysis (see, [18], for proofs and more details).

Theorem 1. Suppose $(V_j)_{j \in \mathbb{Z}}$ be a multiresolution approximation such that the associated function $\phi(x)$ satisfies

$$\exists C \geq 0, |\phi(x)| < C(1 + |x|)^{-3-q},$$

$$\int_{-\infty}^{\infty} x^n \phi(x) dx = 0, \quad \text{for } 1 \leq n \leq q + 1,$$

and also,

$$\exists C' \geq 0, \left| \frac{d^n \phi(x)}{dx^n} \right| < C'(1 + |x|)^{-1-q}, \quad n \leq q.$$

Put $\varepsilon_j = \|f - P_{V_j}(f)\|$. Then for all $(x) \in L^2(\mathbb{R})$, if $0 < s \leq q$ we have $f(x) \in H^s \Leftrightarrow \sum_{j=-\infty}^{\infty} \varepsilon_j^2 2^{2sj} < +\infty$.

Consider a Banach space K and a normed linear space G , and a sequence of operators $T_n: K \rightarrow G$, the sequence has order of approximation $\beta(n)$, i.e., for all $f \in A$, $\|(I - T_n)f\|_G \leq C_f \beta(n)$ if and only if for the operator norm, we have

$$\|(I - T_n)\| \leq C' \beta(n),$$

for some C' and each n .

Definition 2. MRA $\{P_n\}$ or wavelet family ψ yields pointwise order of approximation (or convergence) s in H^r if for any $f \in H^r$, the n -th order approximation $P_n f$ satisfies

$$\|E_n f\|_\infty \equiv \|(I - P_n)f\|_\infty = O(2^{-ns}),$$

as n tends to infinity. It yields the best order of approximation s in H^r if s is the largest number such that this relation holds, for all $f \in H^r$.

Now, by the above results whose constraints are met by the functions of our problem we get,

$$u \in H^2 \Leftrightarrow \sum_{j=-\infty}^{\infty} \varepsilon_j^2 2^{4j} < +\infty.$$

Also, for a set of refinable answers u 's, attained by our method, the order of approximation is $O(2^{2n})$. To

elaborate more, given a smooth function $u \in H^2$ projected over the refinable spaces, i.e. $u = u^1 + u^2$, since the required conditions stated in [19] are satisfied, the existence of a constant C_u is guaranteed so that the error estimation for approximation of u are as follows:

$$\|E_n u\|_\infty \leq C_u 2^{-2n} \|u\|_{H^2},$$

$$\|E_n u\|_\infty = O(2^{-2n}),$$

where C (a shape parameter) depends on the function $u(x, t)$. One must keep in mind that the order of approximation lies at the heart of a simple difference norm that demonstrates the degree of precision, namely, $\|f - P_{V_j}(f)\|$, where $P_{V_j}(f)$ is an approximation for the function f . A classical problem in approximation theory is to estimate the convergence rate of ε_j based on a priori knowledge on the smoothness of $f(x)$, or conversely, derive the smoothness of $f(x)$ out of the convergence rate of ε_j .

It must be noted that starting from finely distributed set of RBF centers our approach leads to the generation of a dense mesh near the boundaries, while a relatively coarse mesh is maintained elsewhere. A highly ill conditioned system will be assigned to the very fine mesh near the boundaries. Furthermore, the method allows the resulted condition number to be lower than a specified value that guarantees a stable solution (for an illustration of nodal distribution in the proposed algorithm, see Figs. 4 and 5). Finally, in comparison to the results of similar mesh free method applied to the same problem, it could be shown that the approximation order of our method, that stems from the assimilation of RBF and wavelet basis equals to $O(2^{2n})$, which surpasses that of the standard RBF that is $O(n \log n)$ as stated in [20].

It implies that our model is more efficient than the sheer RBF. Besides, the method is also faster than Finite Volume Method which converges to the solution as fast as $O(n)$ [21]. Also, Mei and Zhu [22], applied another meshless method, called the Homotopy Perturbation Method to solve the Perona-Malik equation through eliminating the boundary effect and showed that the order of approximation is $O(4^{3j})$, which is obviously slower than ours as it grows polynomially, whereas our method converges exponentially. The fast progressing level set method has also been used to solve Perona-Malik Equation [23] and the authors proved that the order of approximation using this method is $O(h^2)$. Indeed, our method with the order $O(2^{2n})$ is the fastest method among the methods introduced so far and therefore requires the least number of operations to reach the solution.

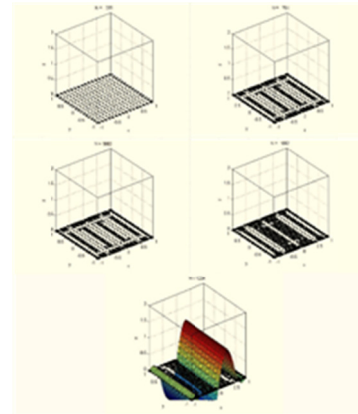


Figure 4. (left) A schematic illustration of nodal distribution produced by the wavelet adaptive technique as well as the chosen RBF centers by the proposed algorithm using multiquadratic function.

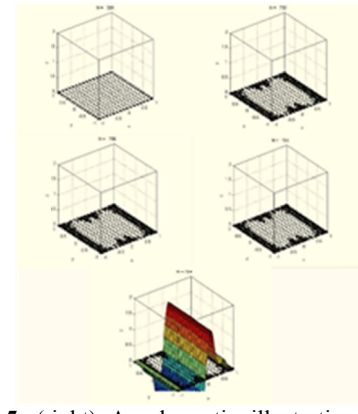


Figure 5. (right) A schematic illustration of nodal distribution produced by the wavelet adaptive technique as well as the chosen RBF centers by the proposed algorithm using Wedland polynomial function.

Discussion

We proposed an adaptive wavelet method to solve the nonlinear Perona- Malik equation and showed that it converges to the solution with a higher approximation order compared to the existing methods. The whole scheme was mainly relied on creating and pertaining the RBF grid by the virtue of the wavelet basis. Nonetheless it must be noted that the method must be tested for the case when the convolution appears inside the gradient itself by Catte-Lion equation [24]. The solution we provided here is akin to a spectrum that contains different layers, each representing certain degree of resolution, and thus the solution can shift from one end of the spectrum to the other. Furthermore, as for any usual RBF method, no mesh has been generated and this advantage could supposedly be applied in 3D cases as

well as the problems that demand re-meshing of the space all along the computations. It should be noted that the larger the time intervals, the more instability the system will experience, but as the comparative computations suggest, instability would be less pronounced if the adaptive wavelet CSRBF method is used.

Conclusion

Finally, our method is fairly optimized and easy to implement. Besides, the wavelet transformations can be engaged more directly in the course of the computation via building a sequence of bounded wavelets to approximate the solution, albeit the ultimate shape of the exact solution is not quite regular and therefore easily prone to fit in.

Acknowledgement

This work was part of the PhD thesis of the first author supported by Tarbiat Modares University.

References

1. Moody J. and Darken C. Fast learning in networks of locally-tuned processing units. *Neural Computation* **1**:281-294 (1989).
2. Yee P. and Haykin S. A Dynamic regularized Gaussian radial basis function network for nonlinear nonstationary time series prediction. *IEEE Signal Processing Society* **47**(9): 2503-2521 (1999).
3. Buhmann M. D. *Radial basis functions*. Cambridge University Press, Cambridge (2003).
4. Uhlir K. and Skala V. Radial basis function use for the restoration of damaged images. *Computer Vision and Graphics*. In: Computational Imaging and Vision book series (CIVI, volume 32) pp. 839-844 (2006).
5. Amattouch M.R. Belhadj and H. Nabila, A modified fixed point method for the Perona-Malik equation, *Journal of Mathematics and System Science* **7**: 175-185 (2017).
6. Guidotti P. Kim Y. and Lambers J. Image restoration with a new class of forward-backward-forward diffusion equations of Perona-Malik type with applications to satellite image enhancement, *SIAM J. Imaging Sci.* **6**: 1416-1444 (2013).
7. Guo Z. Sun J. Zhang D. and Wu B. Adaptive Perona-Malik model based on the variable exponent for image denoising, *IEEE Trans. Image Process* **21**: 958-967 (2012),
8. Mescheder L.M. and Lorenz D.A. An extended Perona-Malik model based on probabilistic models, *J Math Imaging and Vision* **60**: 128-144 (2018).
9. Maiseli B. Msuya H. Kessy S. and Kisangiri M. Perona-Malik model with self-adjusting shape-defining constant, *Information Processing Letters* **137**: 26-32 (2018).
10. Vrankar L. Ali Libre N. Ling L. Turk G. and Runovc. F. Solving moving-boundary problems with the wavelet adaptive radial basis functions method. *Computers & Fluids* **86**: 37-44 (2013).
11. Blu T. and Unser M. Wavelets, fractals, and radial basis functions. *IEEE Transactions on Signal Processing* **50**: 543-553 (2002).
12. Rannacher R. and Wendland W.L. On the order of pointwise convergence of some boundary element methods. Part II: Operators of positive order. *Math. Modeling Numer. Anal.* **22**:343-362 (1988).
13. Larsson E. and Fornberg B. A numerical study of some radial basis function based solution methods for elliptic PDEs. *Computers Math. Appl.* **46**: 891-902 (2003).
14. Meyer Y. *Wavelets and operators*. Cambridge Univ. Press, Cambridge (1992).
15. Mallat S. *A wavelet tour of signal processing*. Academic Press, New York (1999).
16. Unser M. A. and Blu T. A. Comparison of wavelets from the point of view of their approximation error. *Proc. SPIE* 3458. In: Wavelet Applications in Signal and Image Processing VI, ed. A F Laine, M A Unser, A Aldroubi (1998).
17. Debnath L. *Wavelet transforms and time-frequency signal analysis*. Birkhäuser, Boston (2001).
18. Kelly S.E. Kon M.A. and Raphael L.A. Local convergence for wavelet expansion. *J. Func. Anal.* **126**: 102-138 (1994).
19. Zhongying C. Micchelli C.A. and Yuesheng X. A multilevel method for solving operator equations. *Journal of Mathematical Analysis and Applications* **262**: 688-699 (2001).
20. Kamranian M. Dehghan M. and Tatari. M. An image denoising approach based on a meshfree method and the domain decomposition technique. *Engineering Analysis with Boundary Elements* **39**: 101-110 (2014).
21. Handlovíčová A. and Krivá Z. Error estimates for finite volume scheme for Perona-Malik equation. *Acta Math. Univ. Comenianae* **LXXIV**: 79-94 (2005).
22. Mei S.L. and Zhu. D.H. HPM-based dynamic sparse grid approach for Perona-Malik equation. *Scientific World Journal*, 417486 (2014).
23. Rumpf M. and Preusser T. A level set method for anisotropic geometric diffusion in 3D image processing. *SIAM J. Appl. Math.* **62**(5): 1772-1793(2006).
24. Alvarez L. Lions P.L. and Morel J.M. Image selective smoothing and edge detection by nonlinear diffusion. II. *SIAM J. Numer. Anal.* **29**(3):845-866 (1992).